NASA CONTRACTOR REPORT

NASA CR-494

REFRACTION OF SOUND BY JET FLOW OR JET TEMPERATURE

by J. Atvars, L. K. Schubert, E. Grande, and H. S. Ribner

Prepared by

UNIVERSITY OF TORONTO

Toronto, Canada

for

NATIONAL AERONAUTICS AND SPACE ADMINISTRATION • WASHINGTON, D. C. • MAY 1966

NASA CR-494

REFRACTION OF SOUND BY JET FLOW OR JET TEMPERATURE*

By J. Atvars, L. K. Schubert, E. Grande, and H. S. Ribner

*This report is a revised and extended form of paper No. 65-82 "Refraction of Sound from a Point Source Placed in an Air Jet" presented at the AIAA 2nd Aerospace Sciences Meeting, New York, Jan. 25-27, 1965. An earlier abbreviated version was presented in J.A.S.A., Vol. 37, No. 1, 168-170, Jan. 1965.

Prepared under Grant No. NsG-661 by
UNIVERSITY OF TORONTO
Toronto, Canada

for

NATIONAL AERONAUTICS AND SPACE ADMINISTRATION

For sale by the Clearinghouse for Federal Scientific and Technical Information
Springfield, Virginia 22151 – Price $2.00

ACKNOWLEDGEMENT

The authors wish to thank Brij. M. Nayar, who assisted in taking the measurements. The work was supported by Air Force Office of Scientific Research, Grants AFOSR 223-64, and 672-64, by National Research Council of Canada, Grant A 2003, and by National Aeronautics and Space Administration, Grant NsG 661.

SUMMARY

The heart-shaped pattern of subsonic jet noise normally peaks somewhere between 15° and 45° from the axis, depending on conditions, falling off sharply as the axis is approached. Conflicting explanations of this directivity pattern appear in the literature. The present investigation suggests that the deep cleft in the pattern can be attributed mainly to refraction of the sound out of the jet by the velocity and temperature fields. The evidence lies in measurements made of the sound field of a harmonic "point" source placed within a 3/4" dia. air jet. The source is the orifice of a tube about 1/16" i.d. driven through a conical coupling by a horn-type loudspeaker driver; this radiates sound essentially omnidirectionally up to about 15,000 cps. The experiment established the formation of an axial intensity minimum, which appears to be mainly due to refraction. The depth of the refraction valley increases with jet velocity, jet temperature, and sound frequency; a depth corresponding to an intensity reduction of the order of 35 dB is attained at M = 0.9 for 3000 cps.

TABLE OF CONTENTS

I INTRODUCTION

The "heart-shaped" pattern of jet noise (e.g., Fig. 1) peaks somewhere between 15° and 45° from the axis, depending on conditions, falling off sharply as the axis is approached. Conflicting explanations of this directivity pattern appear in the literature [1-8]. Powell [4] and Ribner [5-8] suggest that the axial intensity minimum is due to refraction of the aerodynamically generated sound by the jet velocity and temperature fields. (See also References 9-15.) The difficulty of this problem has limited 'exact' analytical approaches [10-14] to idealized jets of infinite extent, without spreading. The predictions must greatly overestimate the refraction for wavelengths typical of jet noise, which are not small compared with the jet dimensions. Moreover, the use of ray tracing for jets of more realistic shape must be suspect because the velocity variations are large within a wave length.

For these reasons an experimental approach was decided on for the present investigation. The experiment consisted of placing a harmonic "point" source of sound within the flow field of a 3/4" air jet and observing the distortion of its inherently omnidirectional sound field. Four experimental parameters were felt to be of chief importance: jet velocity, jet temperature, source frequency, and source position.

The specialized facility and equipment developed for this investigation are described below.

II EXPERIMENTAL FACILITY

2.1 Anechoic Chamber

All measurements were made in an anechoic chamber (Fig. 2) constructed in the basement of the University of Toronto Institute for Aerospace Studies. The chamber is 13' long by 9'4" wide by 6'10" high as measured between the tips of the 8" deep Fiberglas wedges. A wire grid, spring tension mounted 4" above the wedges, serves as floor. A 1/16" layer of lead sheet on the walls and a "floating" ceiling help to attenuate exterior noise and vibration. The residual background level in the chamber is acceptably low. For test signals above 300 cps (the low frequency cut-off) deviations from the inverse square law for far-field acoustic intensity were of the order of 1 dB to within about 1 foot of the wedge tips.

2.2 Air Jet

The air jet issues from a circular nozzle 3/4" in diameter and can be operated from M = 0 to M = 1. The nozzle contraction was designed to produce a uniform velocity profile at the orifice. The contraction is preceded by a section of 8" pipe about 4' long, housing a heating section and a settling chamber[3]. The heating section, which contains an array of 9 heating coils, has a maximum capacity of 9 kw. A temperature controller linked to a thermocouple in the settling chamber and to a switch in the power supply line provides for automatic maintenance of a preset stagnation temperature. The entire length of the 8" pipe was clad in a heavy layer of asbestos insulation. The maximum exit static temperature attainable was around 600° F at a velocity of 150 fps, and slightly above room temperature for sonic velocity.

The velocity profiles of the jet showed the desired uniformity near the nozzle. Temperature profiles obtained in horizontal traverses were also reasonably uniform; the vertical temperature profile develops a marked non-uniformity at low jet velocities, because of convection of the hottest air to the top of the settling chamber. However, this is believed to have relatively little bearing on measurements made entirely in a horizontal plane containing the jet axis. The jet is located off to one side in the anechoic room in order to maximize the radius of the semi-circular microphone traverse (76 5/8"). The air flow is supplied by a continuously operating compressor and exhausts from the anechoic room through a 2 1/2 foot square duct lined with Fiberglas..

2.3 Harmonic "Point" Source

The sound source utilizes a horn-type loudspeaker driver (University, model I D-60) encased in a triple-walled cylindrical enclosure (Fig. 4). This enclosure is designed to attenuate sound radiated from the driver casing by about 60 dB. The "point" source is the orifice of a 1/16" i.d. hypodermic tube coupled to the driver unit by a section of pipe containing a conical contraction. The tip of the tube was bent to point directly downstream in the jet. One version of the tube was fitted with a balsa wood airfoil fairing to minimize turbulence in the wake, but this was found to have no measurable effect on experimental results.

Circular sound pressure level traverses at various frequencies showed that in the absence of a jet the source radiates essentially omnidirectionally up to about 15000 cps, as expected from theory [16].

Various tests indicate that the stem of the hypodermic tube is not a significant secondary source of sound. For example, blocking of the orifice caused a drop in SPL of more than 20 DB at frequencies between 1000 cps and 10,000 cps. The change in net impedance seen by the driver is believed to be negligible in this test; this implies negligible change in internal levels, hence in stem vibration.

2.4 Instrumentation

The experimental arrangement and instrumentation are shown in Fig. 5. For ease of operation and also in order to reduce the number of sound reflecting objects in the anechoic chamber, nearly all the instruments and controls are located in the adjacent room.

An Altec Lansing type 21-BR-150 condenser microphone shielded by a fabric mesh windscreen was used for all measurements. The microphone is attached to a boom pivoted directly above the orifice of the sound source. The source-to-microphone distance of more than 6' was sufficient for far-field measurements at the frequencies considered. The microphone signal was passed through a General Radio sound level meter to a Muirhead wave analyzer. The analyzer effectively served as a narrow band filter with a band width equal to 2% of the centre frequency. At moderate frequencies (< 4000 cps) and moderate Mach numbers (< 0.5) the pure tone overrode the jet noise in this bandwidth. For $M > 0.5$ the Muirhead wave analyzer was replaced by a Princeton Applied Research Model JB-5 Lock-In Amplifier in order to extract the signal from the higher noise background (cf. 3.4).

The frequency of the sound source was selected on a Muirhead decade audio oscillator whose output was passed through a power amplifier to the driver unit.

III EXPERIMENTAL METHOD

3.1 General Procedure

For a given microphone position and source frequency the sound pressure level at the microphone was observed on the analyzer decibel scale. Then, while the power input into the source was left unaltered, the jet was turned on and the new reading on the analyzer recorded. The difference between the two readings gave the sound pressure level (SPL) reduction. This change in SPL was then normalized with respect to the value at 90°, since in this position there should be no appreciable change in readings for the "jet off", "jet on" cases according to simple refraction theory (ray acoustics).

3.2 Jet Velocity

The source frequency was kept constant at an effective value of 3000 cps (actually results were averaged for 2900, 3000 cps to suppress scatter) while the jet Mach number was varied from 0.1 to 0.95 for a room temperature jet. The SPL reductions were plotted as a function of Mach number for each angular position of the microphone (as in Fig. 6). From the family of curves thus obtained, cross-plots of the directivity patterns were made (Fig. 7). For Mach numbers above 0.5 the filtered jet noise overrode the pure signal.

In this regime the source signal was at first extracted by a correlation technique. Upon acquisition of a lock-in amplifier (cf. 2.4) it was found that substantially better discrimination against the noise background was obtained; this was evidenced by lower signal minima at $\theta = 0$. The lock-in amplifier was used for all the present data for Mach numbers above 0.5.

In Fig. 6 it is seen that the experimental readings obtained with the lock-in amplifier for velocities higher than Mach = 0.5 show increasing deviation from the straight line indicated by low velocity measurements. This discrepancy may be explained if a cusp-like shape of the refraction valley is assumed. The measured axial intensity minimum is then the average intensity over the area of the microphone. The corrected curve in Fig. 6 was calculated by assuming the following intensity variation near the jet axis

$$\langle p^2 \rangle \sim A + B \sqrt{\theta} + C\,\theta$$

The details are indicated in the Appendix.

3.3 Jet Temperature

The SPL reduction was determined for a sequence of jet temperatures from ambient to 500°F. The source was 2D from the nozzle and the jet velocity was maintained at 223 ft/sec. As for the determination of velocity dependence, frequencies of 2900, 3000 and 3100 cps were used and the results averaged. The jet temperature was varied through the complete range at each angular position (e.g. Fig. 8). Crossplotting at selected temperatures then gave the directivity patterns shown in Fig. 9.

3.4 Source Frequency

The jet Mach number was kept constant at 0.3; with the jet at room temperature and with the sound source located on the jet axis 2D downstream of the nozzle, the frequency of the pure tone from the sound source was varied in 100 cps steps from 900 cps up to 7100 cps. From the family of curves with angular position as parameter cross-plots of the directivity patterns were made as before. Figs. 10 and 11 show some typical results for the effect of frequency on directivity.

3.5 Source Position

(a) Axial Position

For each axial position the jet was maintained at ambient temperature and Mach 0.15. The source frequency was again varied from 900 cps to 7100 cps. The axial distances of the source from the nozzle used for this investigation were 1D, 2D, 4D and 8D. The shifts in source position were made both at constant source-to-microphone distance and at constant nozzle-to-microphone distance. Some results for the 1D and 8D positions are shown in Fig. 12.

(b) Radial Position

Both positions within the jet and entirely outside the jet have now been investigated. Extensive data were obtained with the source 2D downstream of the nozzle and displaced 1/2D from the jet axis. This radial position coincides approximately with the region of maximum aerodynamic noise generation. Directivity patterns were determined by cross-plotting from frequency dependence curves (e.g. Fig. 13) obtained for successive azimuthal microphone stations. Since the traverse of the microphone boom was limited to angles with the jet axis between about -7° and 120°, the second half of each directivity pattern was obtained by moving the source horizontally to the diametrically opposite point in the mixing region and plotting the mirror image. A similar procedure was followed for source positions outside the jet. Directivity curves are shown in Figs. 14 and 15, corresponding to source positions 1/2D and 2D off the jet axis respectively.

IV RESULTS

From examination of the directivity patterns of Figs. 7, 9, and 11, it is immediately obvious that the spherically symmetric directivity pattern of the sound source is locally distorted by the jet velocity and temperature fields, forming an axial intensity minimum. This deep valley in the directivity pattern is attributed mainly to refraction. It is further noted that the refraction valley deepens as either the jet velocity (Fig. 7), the jet temperature (Fig. 9) or the source frequency (Fig. 11) is increased. Just such behaviour is to be expected for refraction by jet velocity and temperature gradients of limited spatial extent.[4-8]

Scattering of the sound by the jet turbulence could contribute to the measured effects on directivity, but it is thought that the contribution is probably small. The theoretical argument notes that the acoustic wave lengths are mismatched to the turbulence scales, being much larger for the most part.[17,18] Experimentally, the introduction of a series of canted airfoil type vortex generators at the nozzle failed to make any measurable change in the directivity contours, although a noticeable increase in the volume of the region of strong turbulence is presumed to have resulted.

An unexpected result was that variation of the axial source position between 1D and 8D (Fig. 12) produced no experimentally significant change in the directivity patterns from 1000 cps to at least 6000 cps. (The behaviour above about 6000 cps is uncertain because of the large amount of scatter.) Of course this applies only in the range of positions investigated, and a weakening of the valley must take place eventually as the source is moved downstream.

When the "point" source was moved laterally away from the jet axis, directivity curves with marked asymmetry (Figs. 14 and 15) were obtained. The asymmetry increases with source frequency and distance from the axis. For source positions well outside the jet (e.g. 2D) the intensity peak on the same side of the jet as the source becomes very prominent. This phenomenon can be regarded as reflection by the jet. At the same time the reduction in valley depth becomes considerable (11 dB in the particular case shown) as can be seen by comparing with results for the same Mach number but with the source on the axis (Fig. 10). On the other hand, the depth of the downstream intensity minimum is reduced only slightly (2 dB) by a (1/2)D shift off the axis. This suggests that an axially symmetric distribution of sources at a radius of (1/2)D from the jet axis will give much the same directivity pattern as a source located on the axis. To investigate this possibility somewhat more closely, the following comparison was made. The points on the directivity pattern for 7000 cps, with the source in the off-axis position, were converted to intensity ratios. The intensities for the two lobes of the pattern were then averaged, and the average expressed in decibels. This average directivity pattern was then superposed on the corresponding directivity pattern with the source on the jet axis. The result is shown in Fig. 16. As noted before, the refraction minimum is reduced 2 dB by the outward displacement of sources. At larger angles the averaged points fall slightly below the centred-source pattern, but only by about .5 dB.

V DISCUSSION

Reflection of sound by the experimental apparatus and the anchoic chamber itself could not be entirely eliminated, even by careful wrapping with Fiberglas of all equipment and addition of a layer of soft Fiberglas batting over the protective wire mesh on the wedges (Fig. 2). Consequently considerable scatter of the data points occurred, especially for measurements near the jet axis at high frequencies. There the sound pressure levels were reduced to values which could be of the same order of magnitude as the spurious reflected signals. It is for this reason that the SPL reduction at any frequency was estimated by averaging results for three successive frequencies 100 cps apart. For example, each point in Fig. 6 represents the average of results for the nominal frequency and two frequencies 100 cps to either side of it. This running average is a valid representation of experimental results, since the experimental graphs are virtually straight lines and the averaging interval is only a small segment of each line. This method of plotting reduced scatter roughly to half.

The immediate environment of the source orifice is different for the "jet on" and "jet off" conditions in that orifice pressure is reduced by the air flow. This effect, which in some of the measurements may have changed the power output of the source, could not have affected results appreciably since normalization with respect to 90° was employed. Also, it is clear from the measurements taken with the source entirely outside the jet that the distortion of the source directivity patterns cannot be attributed to a direct alteration of the source behaviour by the air flow over it.

Fig. 11 shows that some of the directivity curves do not attain positive values to compensate for the refraction valley. (Note that only small positive values are needed there, because of the $\sin\theta$ weighting required by solid angle considerations). This gives then an apparent violation of acoustic energy conservation. However, for the measurements represented in Figs. 7, 9 and 15 positive values were attained; it may be that a refinement in the instrumentation and technique is all that is required for consistency in this respect.

The observation that directivity patterns are virtually independent of the axial position of the source up to at least eight diameters at first seems in conflict with the concept of refraction by the segment of the jet flow lying between the source and the microphone. However, the wavelengths associated with the frequencies used were of the same order of magnitude as the dimensions of the jet itself; thus diffractive effects are strong and the entire flow field, rather than any portion of it, will tend to distort the sound field of the source. Hence it seems plausible that the directivity pattern should be only a weak function of source position within limits.

Experimental work is being continued to provide more complete data and to clarify some of the results discussed above.

VI CONCLUSIONS

The sound pattern of a harmonic "point" source placed in an air jet was found to be distorted from spherical symmetry so as to exhibit a marked dimple or valley. This valley in the directivity pattern is attributed mainly to refraction, the sound rays being bent away from the axis, out of the flow. The depth of the valley increases with jet velocity, jet temperature, and sound frequency, as indicated qualitatively by theory. This valley behaviour for the injected source of sound is similar to that for the turbulence-generated jet noise in given frequency bands. Hence it is concluded that the characteristic valley observed in jet noise directivity patterns is due mainly to refraction.

APPENDIX

Correction For Finite Microphone Size

The directivity curves appear to approach a cusp at the minimum ($\theta = 0$) as either Mach number (Fig. 7) or frequency (Fig. 11) is increased. The averaging effect of the finite microphone size can be significant over such a cusp. We assume that in the general vicinity of the cusp the mean square pressure ratio (P. R. $\equiv \langle p^2 \rangle \; / \; \langle p^2 \rangle$ jet off) is of the form

$$\text{P.R.} = A + B\sqrt{\theta} + C\,\theta \qquad (1)$$

as measured with an ideal 'point' microphone. If the microphone subtends a small cone angle $2\theta_o$ when the source-to-microphone vector $\underline{R}$ is set at $\theta = 0$, then the average over the microphone face is to a close approximation

$$\langle \text{PR} \rangle_{\theta_o} = A + \frac{4}{5} B \sqrt{\theta_o} + \frac{2}{3} C\,\theta_o \qquad (2)$$

On the other hand, when the microphone has moved well off the cusp, it is easy to justify that the average should be essentially the ideal value at the microphone center, given by (1).

Accordingly microphone responses at three angles may be selected to give the following system of equations:

$$\theta = 0: \qquad \langle \text{P.R.} \rangle_{\theta_o} = A + \frac{4}{5} B \sqrt{\theta_o} + \frac{2}{3} C\,\theta_o$$

$$\theta = \theta_1: \qquad \text{P.R.} = A + B\sqrt{\theta_1} + C\,\theta_1$$

$$\theta = \theta_2: \qquad \text{P.R.} = A + B\sqrt{\theta_2} + C\,\theta_2$$

These may be solved simultaneously to give A, the 'corrected' mean square pressure ratio at $\theta = 0$ (cf. (1)).

The effective diameter of the microphone was taken to include an allowance for the measured vibration due to turbulent buffeting. The data were:

microphone diameter	0.5 in.
vibration amplitude (approx.)	0.5 in.
effective diameter	1.0 in.
source-microphone distance, R	76 5/8 in.
angle subtended, $2\theta_o$	0.75°

For M $>$ 0.5 directional traverse data were available only for M = 0.6 and M = 0.9. These were employed in (3) as follows, noting that Δ SPL = $10 \log_{10}(P.R.)$:

M = 0.6

θ^o	Δ SPL, dB (as read)	Δ SPL, dB (corrected)
0	- 22.1	- 23.6 = $10 \log_{10} A$
3	- 19.0	- 19.0
5	- 17.9	- 17.9

M = 0.9

θ^o	Δ SPL, dB (as read)	Δ SPL, dB (corrected)
0	- 30.2	- 35.5 = $10 \log_{10} A$
4	- 24.8	- 24.8
6	- 23.9	- 23.9

These results are exhibited in Figs. 6 and 7.

ADDENDUM TO UTIAS TECHNICAL NOTE NO. 109 (MAY, 1965)

Atvars, J., Schubert, L.K., Grande, E., and Ribner, H.S., "Refraction of Sound by Jet Flow or Jet Temperature"

REFERENCES

(Note: citation of Reference 3 on the bottom line of p. 1 is in error and should be ignored.)

1. Lighthill, M.J. — On Sound Generated Aerodynamically II: Turbulence as a Source of Sound, Proc. Roy. Soc. A222, 1-32 (1954).

2. Lighthill, M.J. — The Bakerian Lecture, 1961. Sound Generated Aerodynamically, Proc. Royal Soc. A267, 147-182 (1962).

3. Lighthill, M.J. — Jet Noise, Wright Brothers Lecture, AIAA Jour. 1, No. 7, 1507-1517 (July 1963).

4. Powell, A. — Survey of Experiments on Jet Noise, Aircraft Engineering 26, 2-9 (1954).

5. Ribner, H.S. — New Theory of Jet-Noise Generation, Directionality and Spectra, J. Acoust. Soc. Amer. 31, 245-246(1959).

6. Ribner, H.S. — Aerodynamic Sound from Fluid Dilations - A Theory of Sound from Jets and Other Flows, U. of Toronto, Institute for Aerospace Studies, UTIA Rep. 86 (AFOSR TN 3430) (1962).

7. Ribner, H.S. — On Spectra and Directivity of Jet Noise, J. Acoust. Soc. Am. 35, No. 4, 614-616 (Apr. 1962).

8. Ribner, H.S. — The Generation of Sound by Turbulent Jets, Advances in Applied Mechanics, Vol. VIII, Acad. Press (N.Y. and London, 1964).

9. Ribner, H.S. — Reflection, Transmission, and Amplification of Sound by a Moving Medium, J. Acoust. Soc. Amer. 29, 435-441 (1957).

10. Gottlieb, P. — Acoustics in Moving Media. Ph.D. Thesis, Physics Dept., Mass. Inst. of Tech. (1959), also Sound Source Near a Velocity Discontinuity, J. Acoust. Soc. Amer. 32, 1117-1122 (1960).

11. Moretti, G., Slutsky, S. — The Noise Field of a Subsonic Jet, Gen. Appl. Sci. Labs., GASL Tech. Rep. No. 150 (AFOSR TN-59-1310) (1959).

12. Slutsky, S., Tamagno, J. — Sound Field Distribution about a Jet. Gen. Appl. Sci. Labs., Tech. Rep. 259 (AFOSR TN 1935) (1961).

13. Slutsky, S. — Acoustic Field of a Cylindrical Jet Due to a Distribution of Random Sources or Quadrupoles, Gen. Appl. Sci. Labs., Tech. Rep. 281 (1962).

14. Cheng. S. — On the Aerodynamic Noise of a Turbulent Jet, Jour. Aerospace Sci., Vol. 28, No. 4, pp. 321-331 (Apr. 1961).

15. Mollö-Christensen, E., Narasimha, R. — Sound Emission from Jets at High Subsonic Velocities, Jour. Fluid Mech., Vol. 8, No. 1, pp. 49-60 (1960). (See also earlier version as M I.T. report.)

16. Beranek, L.L. — "Acoustics", McGraw-Hill, New York (1954), pp. 103-104.

17. Lighthill, M.J. — On the Energy Scattered from the Interaction of Turbulence with Sound or Shock Waves, Proc. Cambr. Phil. Soc. 49, Part 3, 531-551, 1953.

18. Müller, E.A. Matschat, K.R. — The Scattering of Sound by a Single Vortex and by Turbulence, U.S. Air Force Off. of Scient. Res., AFOSR-TN-59-337 (Jan. 1959).

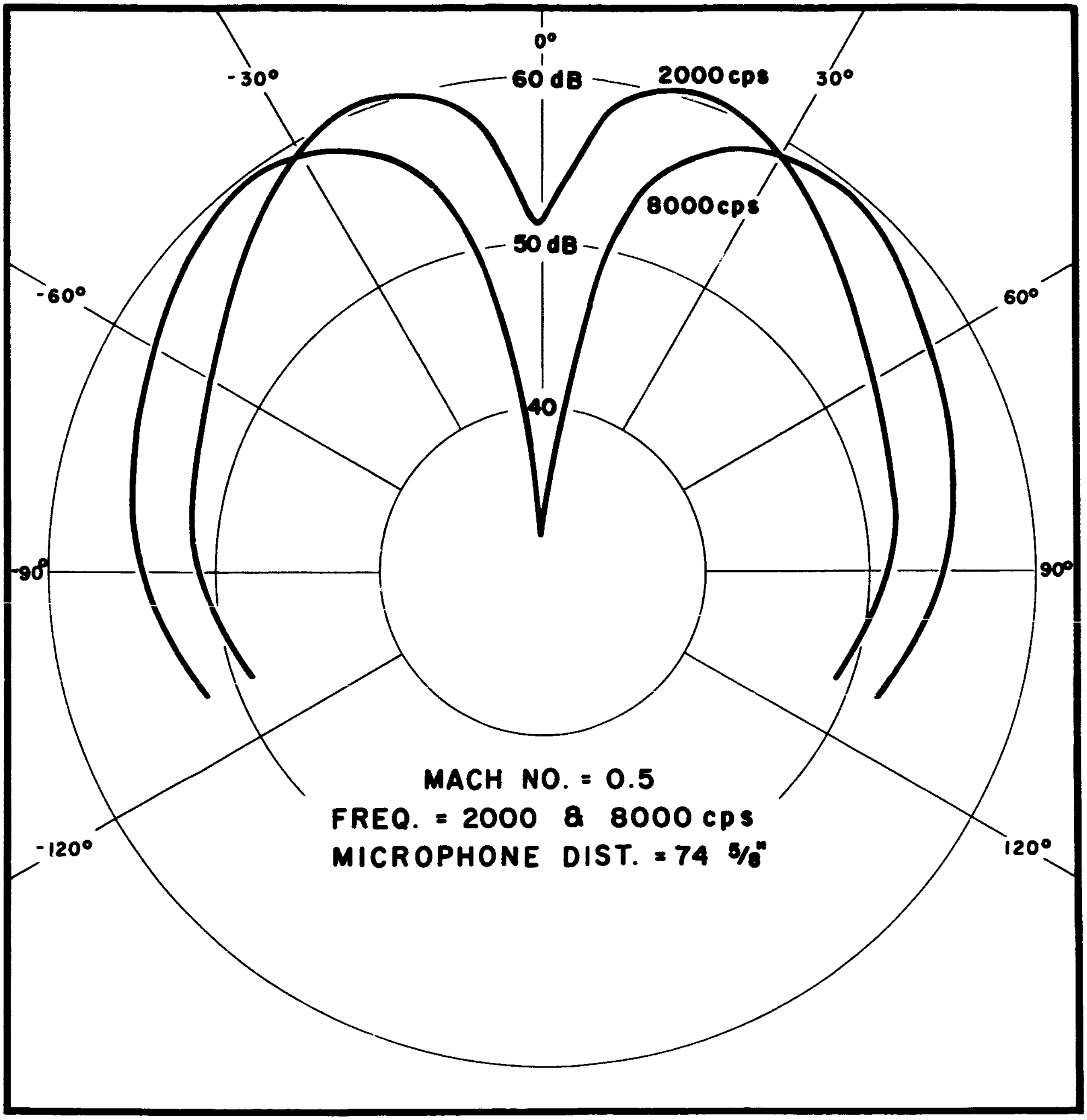

FIG. 1a. JET NOISE DIRECTIVITY FOR 3/4" AIR JET

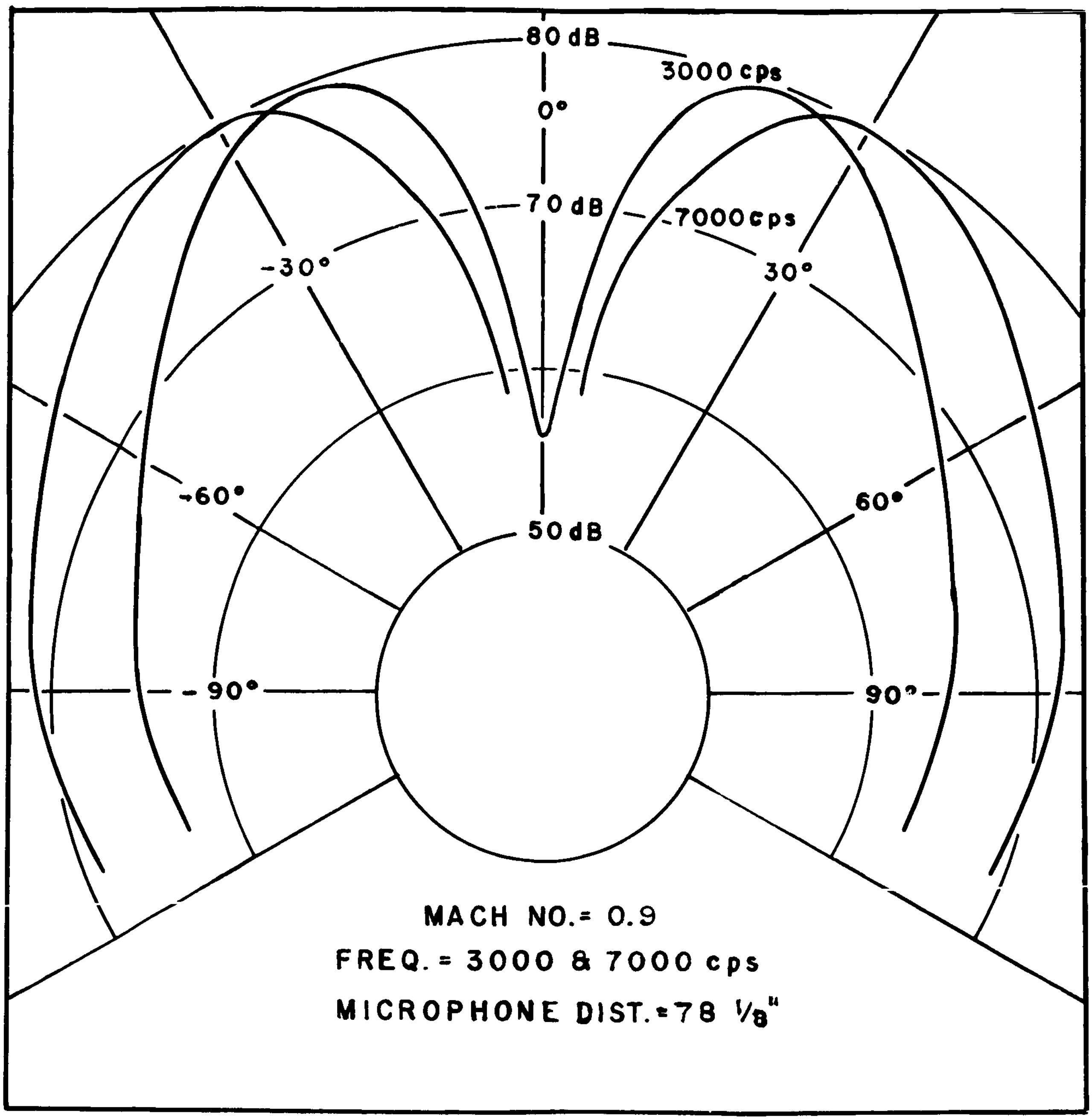

FIG. 1b. JET NOISE DIRECTIVITY FOR 3/4" AIR JET

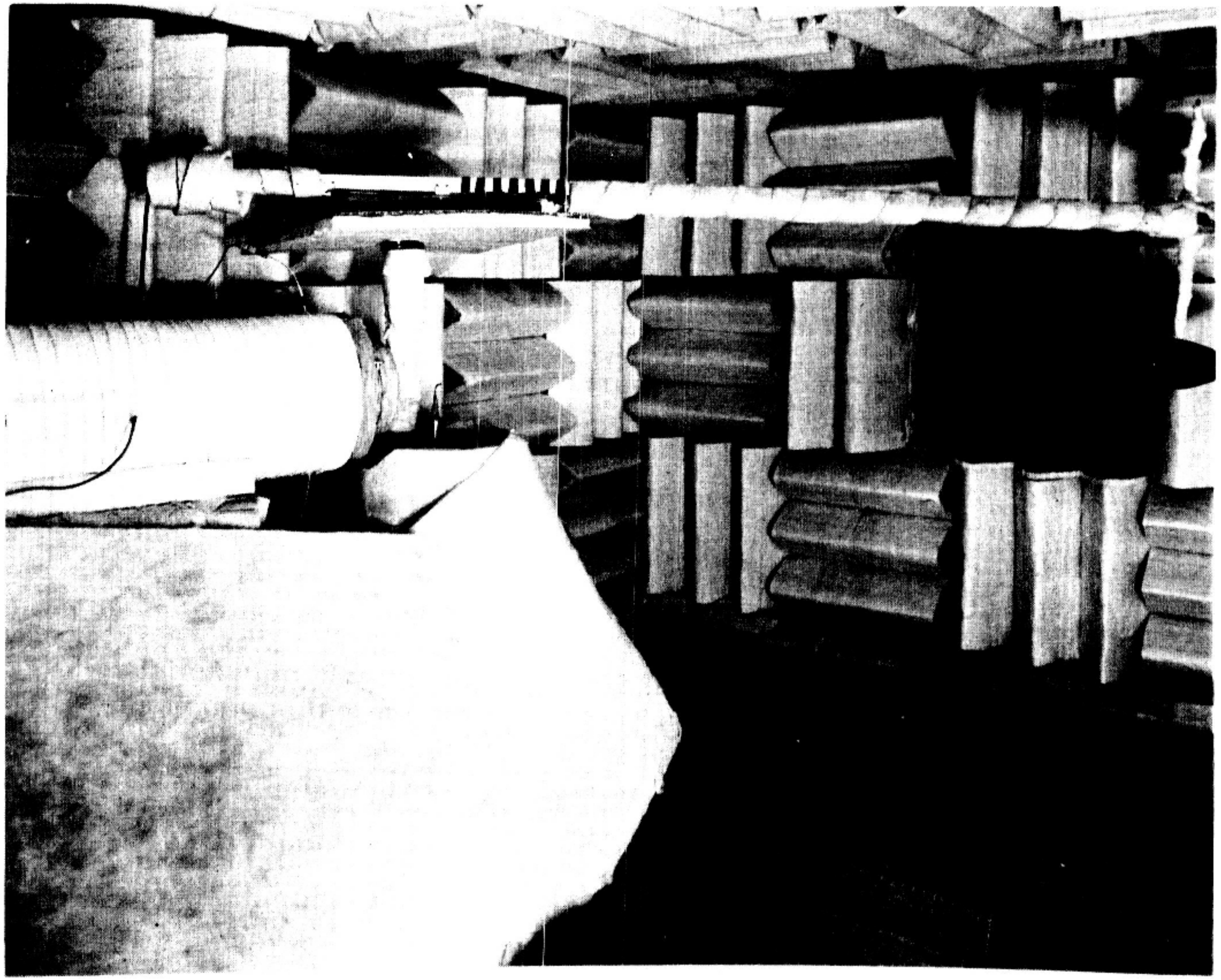

FIG. 2. VIEW OF ANECHOIC ROOM SHOWING JET AND "POINT" SOURCE ON LEFT AND SHIELDED MICROPHONE ON FAR RIGHT.

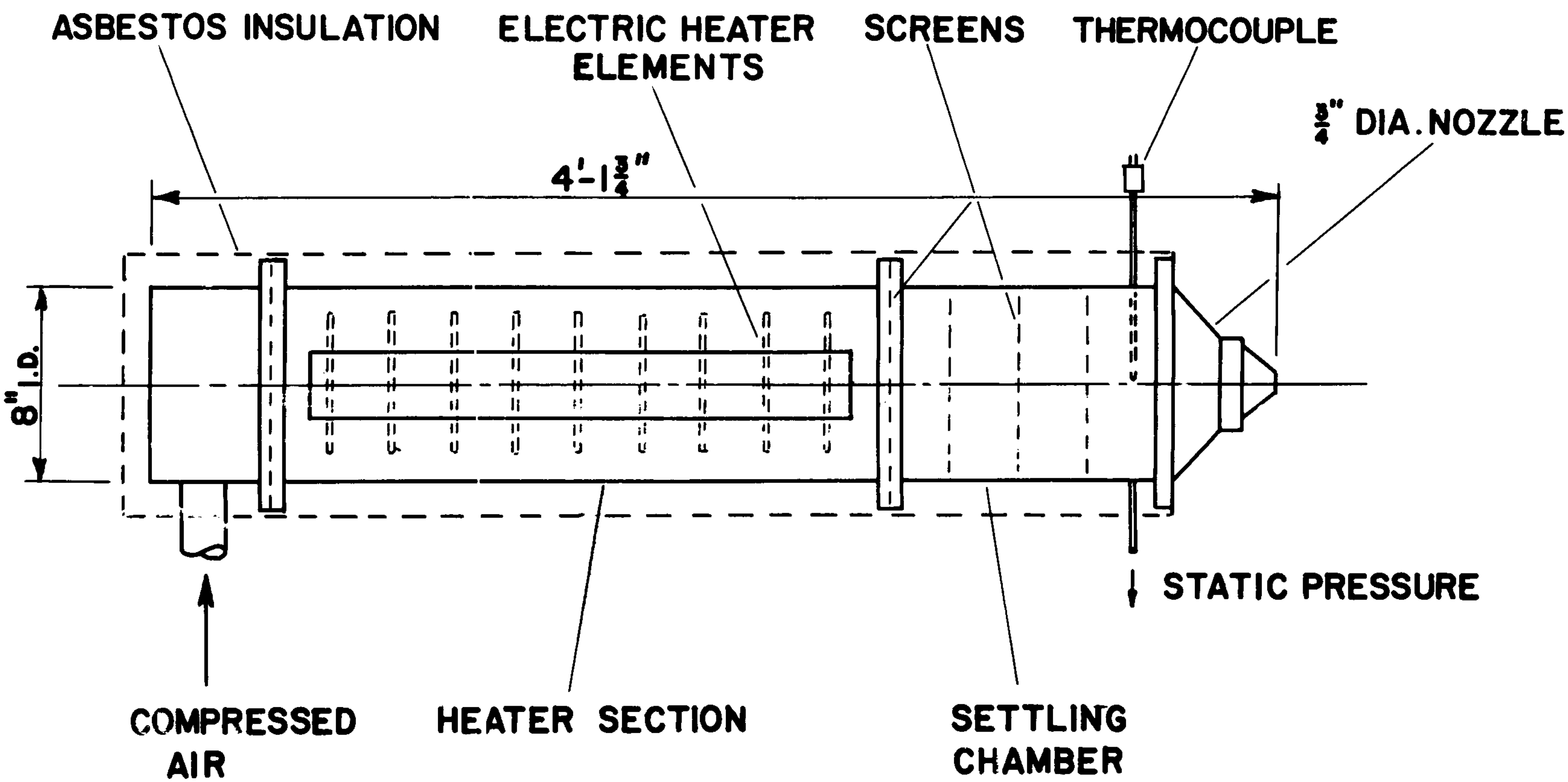

FIG. 3. 3/4" JET FACILITY

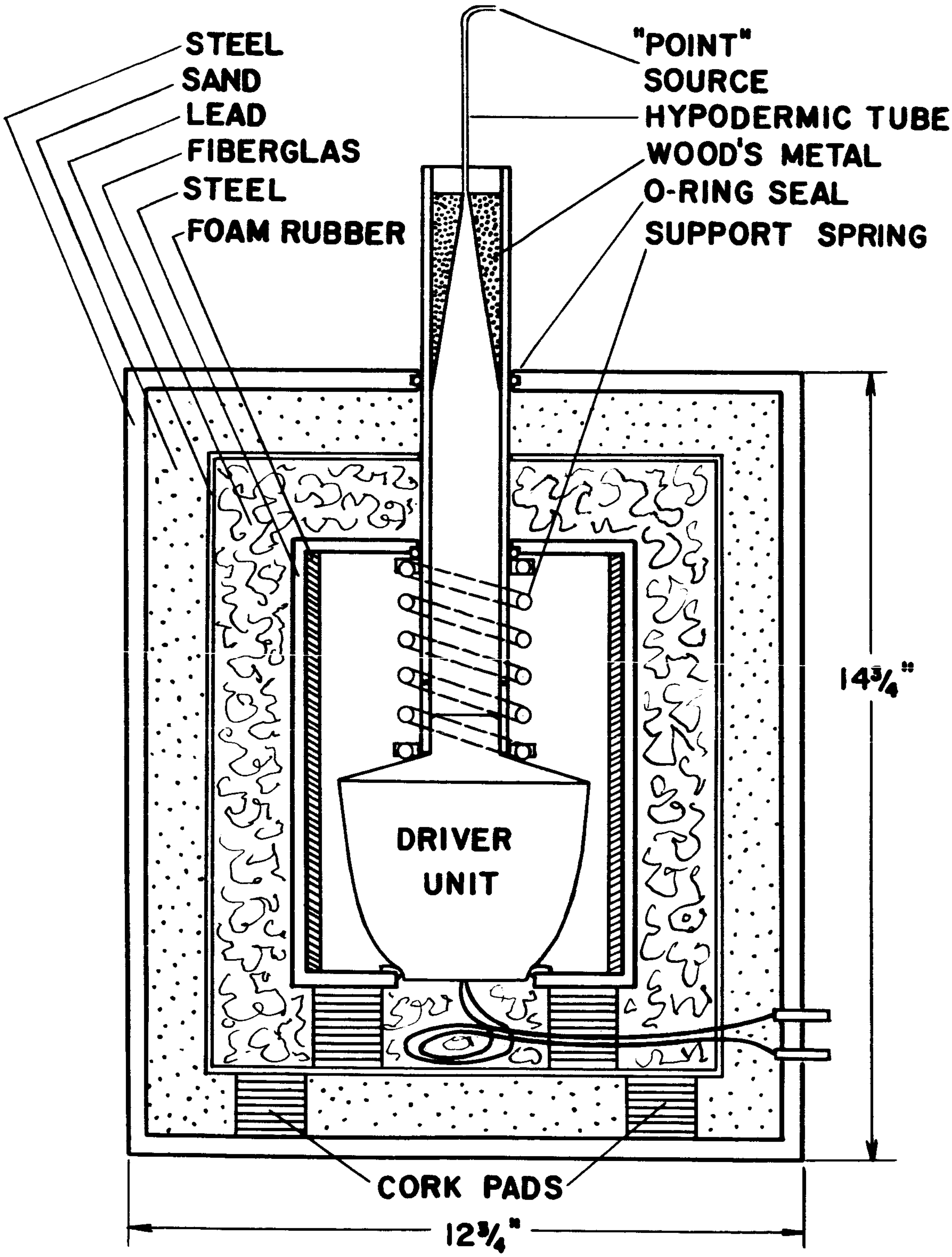

FIG.4. SOUND SOURCE

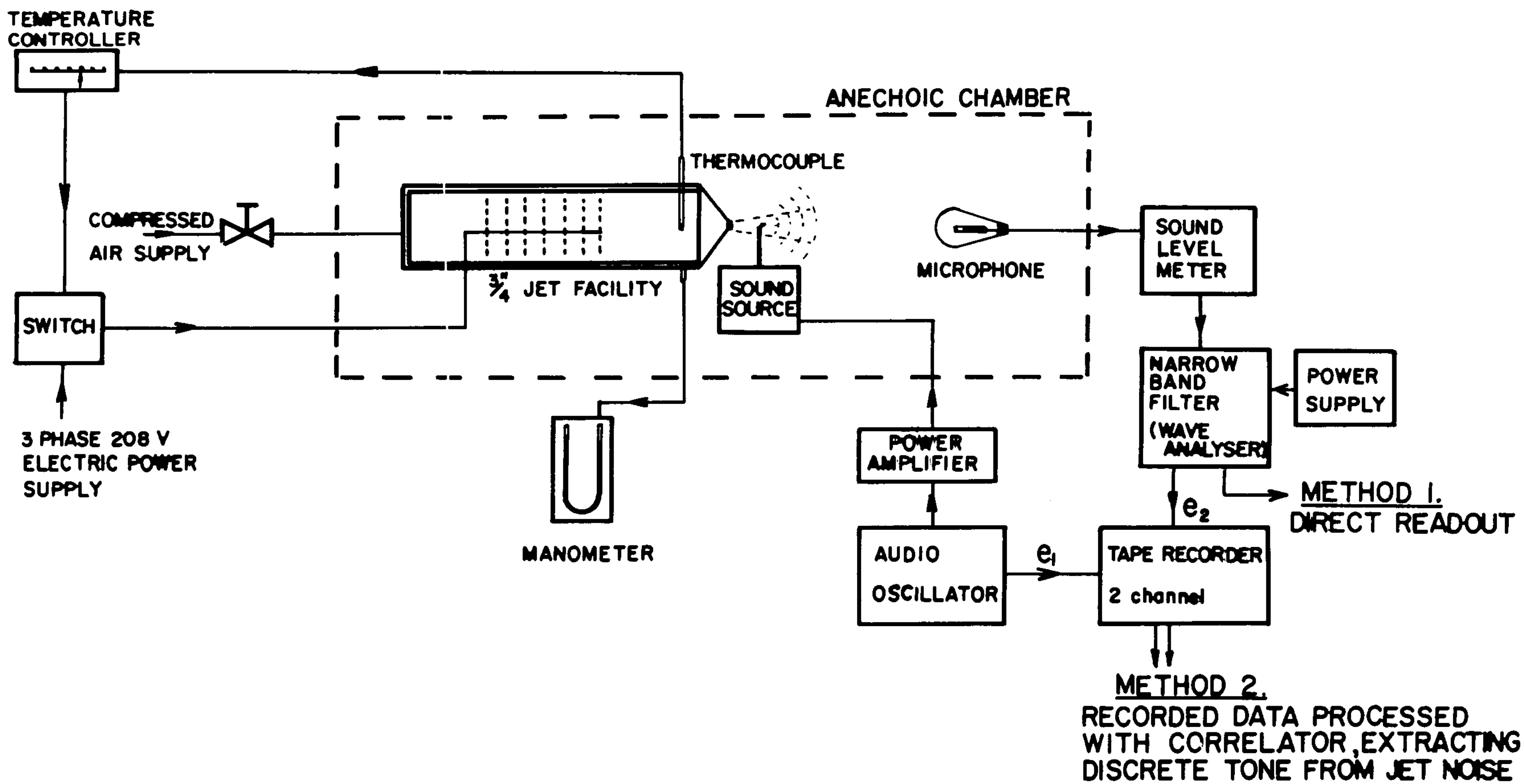

FIG. 5. EXPERIMENTAL ARRANGEMENT AND INSTRUMENTATION.

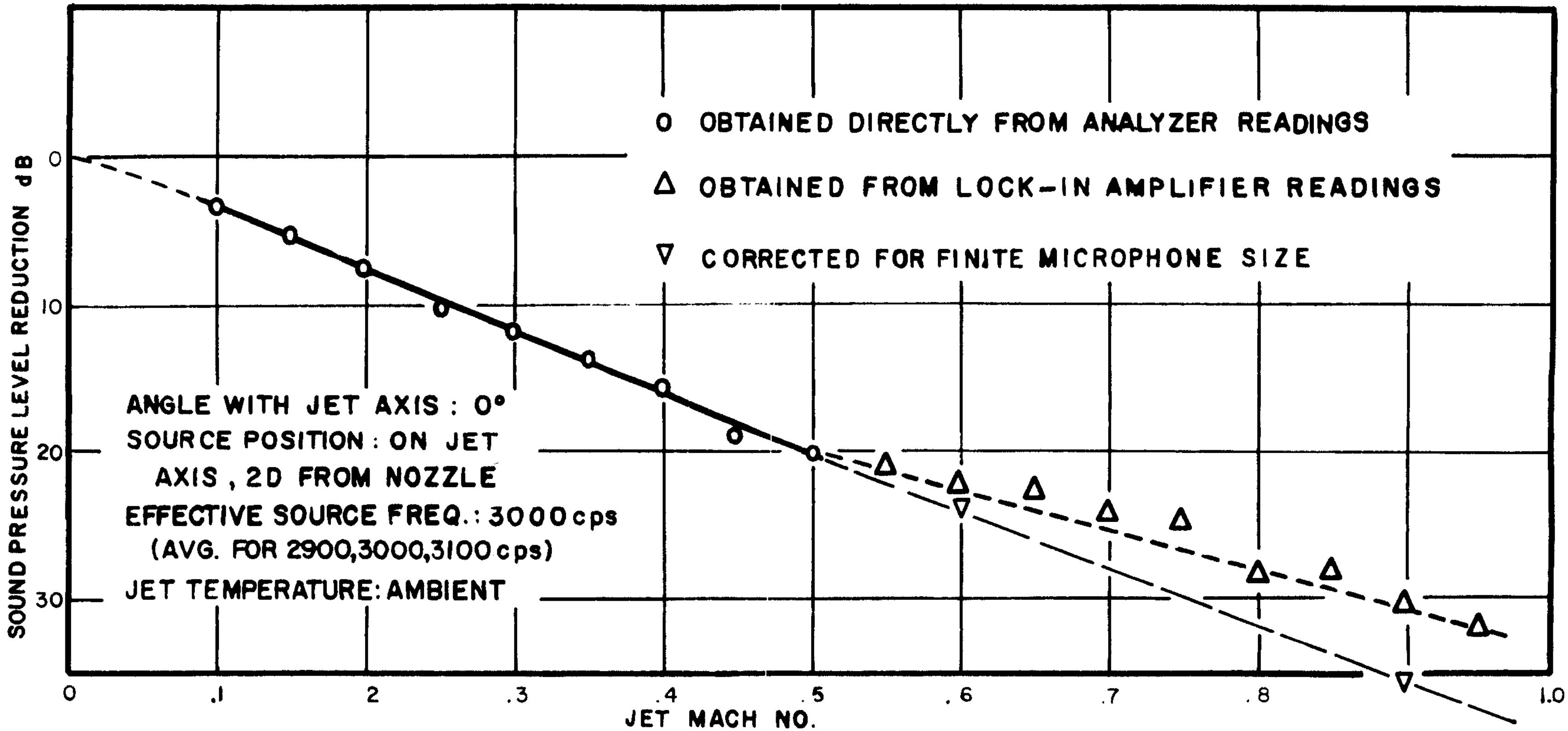

FIG. 6. VELOCITY DEPENDENCE OF REFRACTION

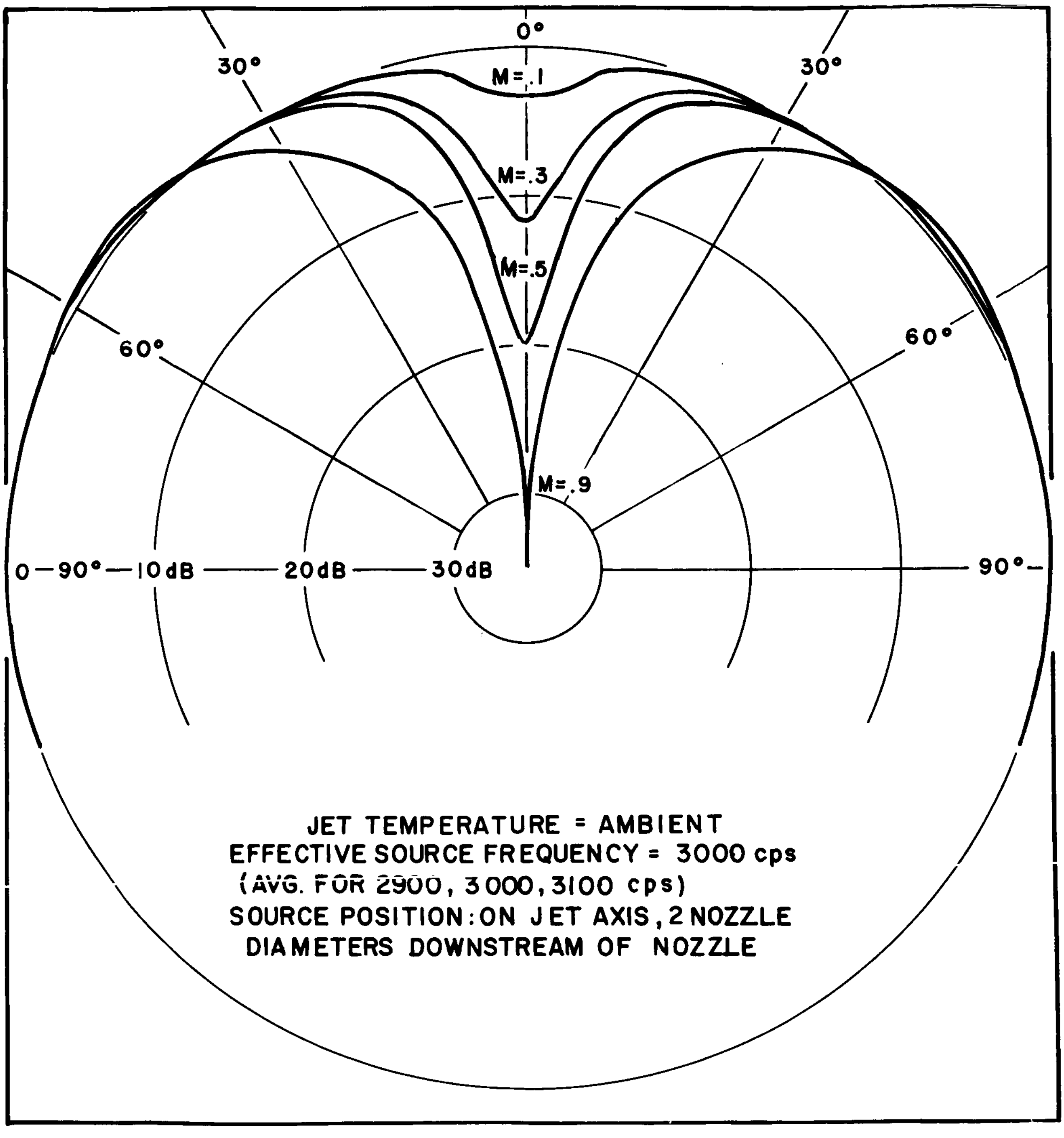

FIG. 7. EFFECT OF JET VELOCITY ON DIRECTIVITY

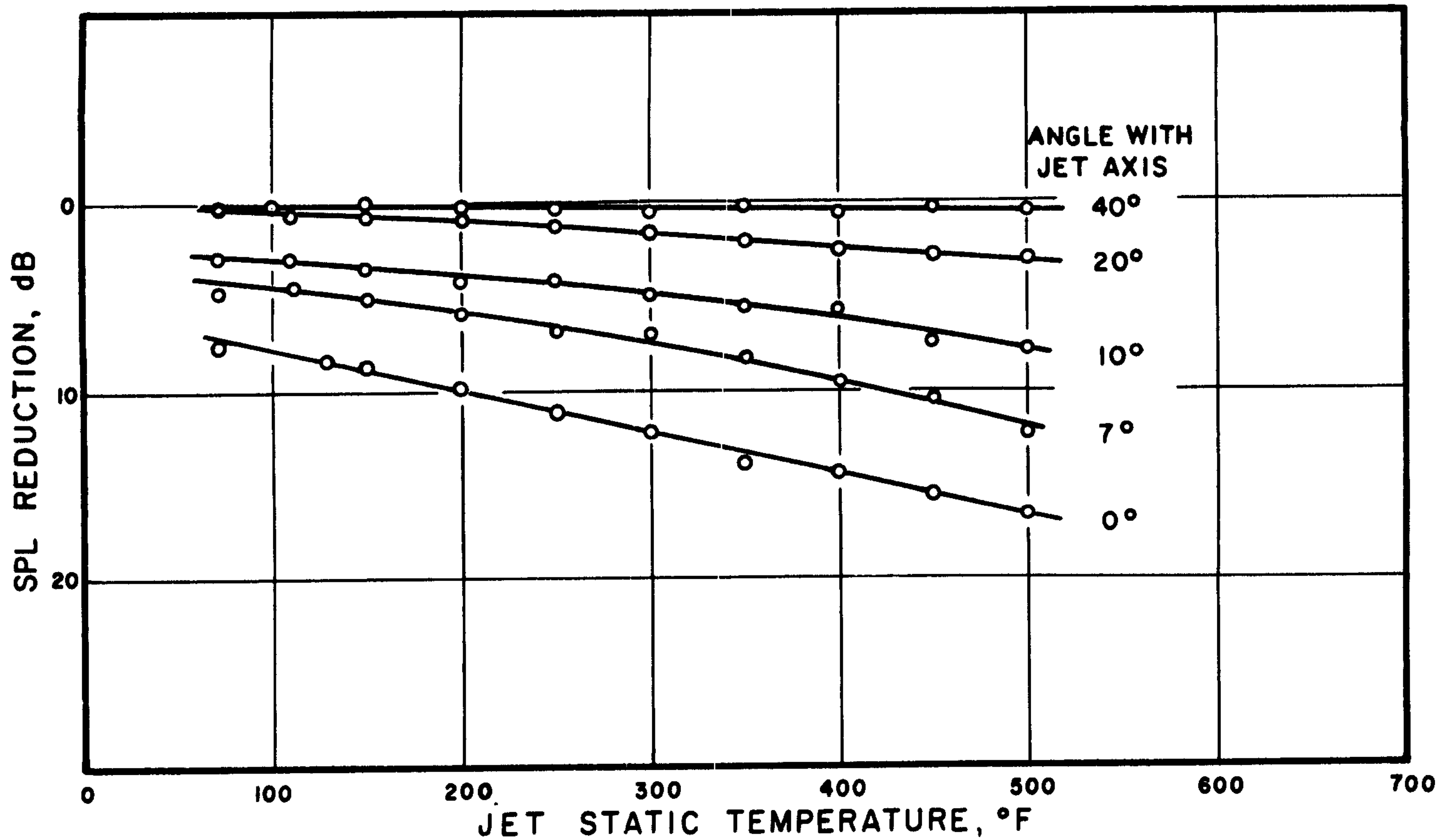

FIG. 8. TEMPERATURE DEPENDENCE OF REFRACTION

EACH POINT AVERAGED FOR 2900, 3000, 3100 cps; V = 223 ft/s

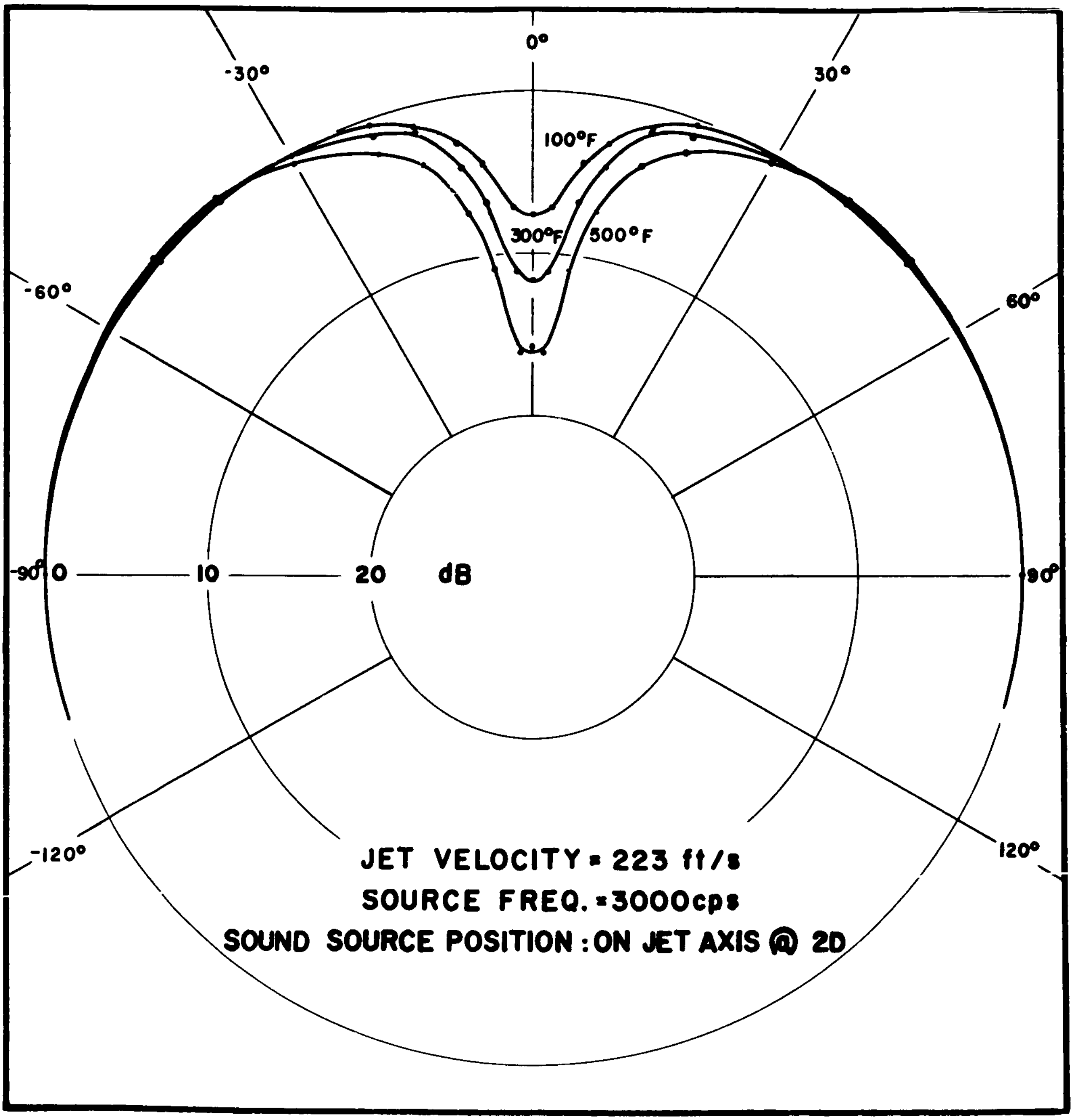

FIG. 9. EFFECT OF JET TEMPERATURE ON DIRECTIVITY

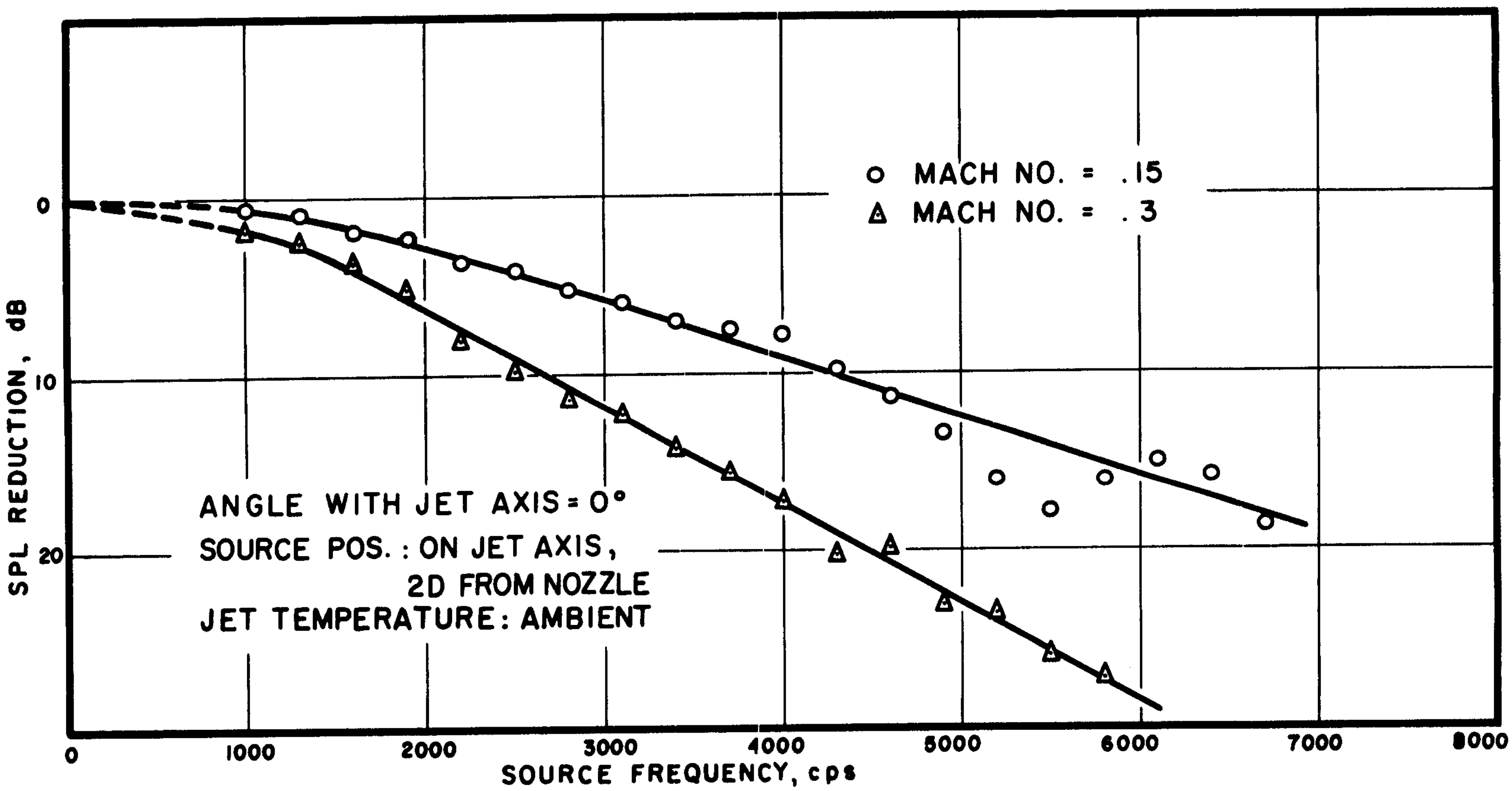

FIG. 10. FREQUENCY DEPENDENCE OF REFRACTION

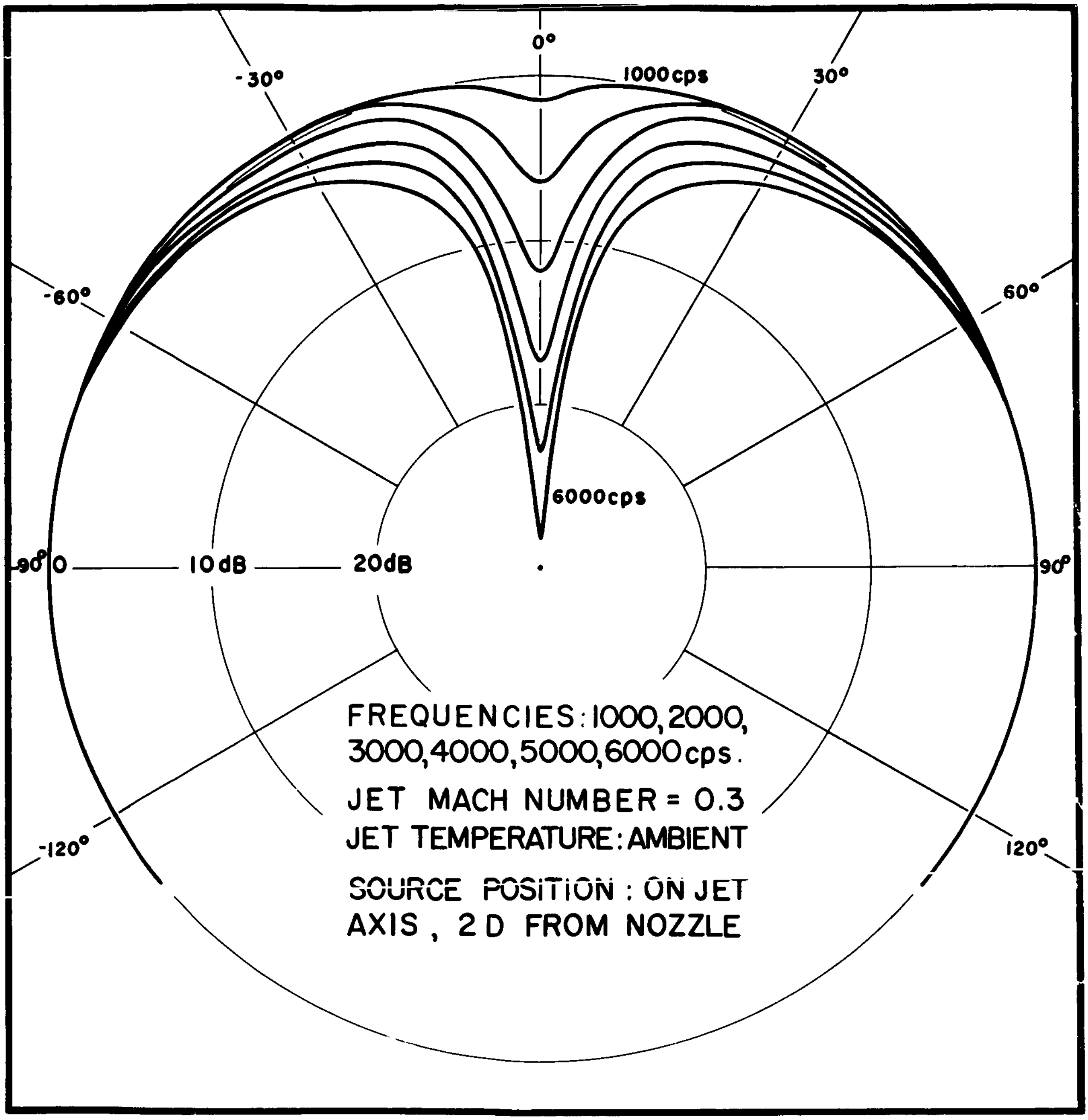

FIG.11. EFFECT OF SOURCE FREQUENCY ON DIRECTIVITY

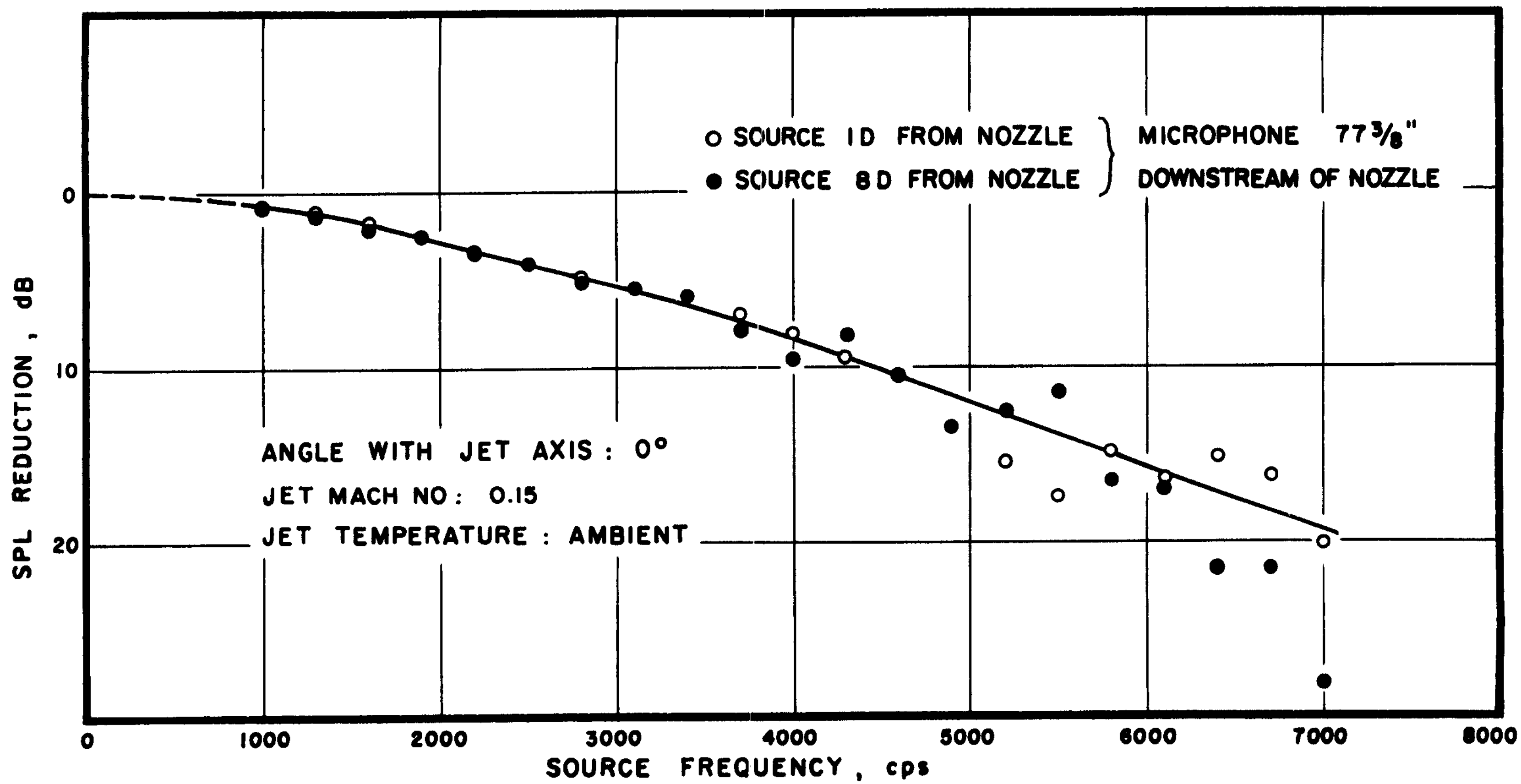

FIG 12. EFFECT OF VARYING SOURCE POSITION WITH MICROPHONE STATIONARY

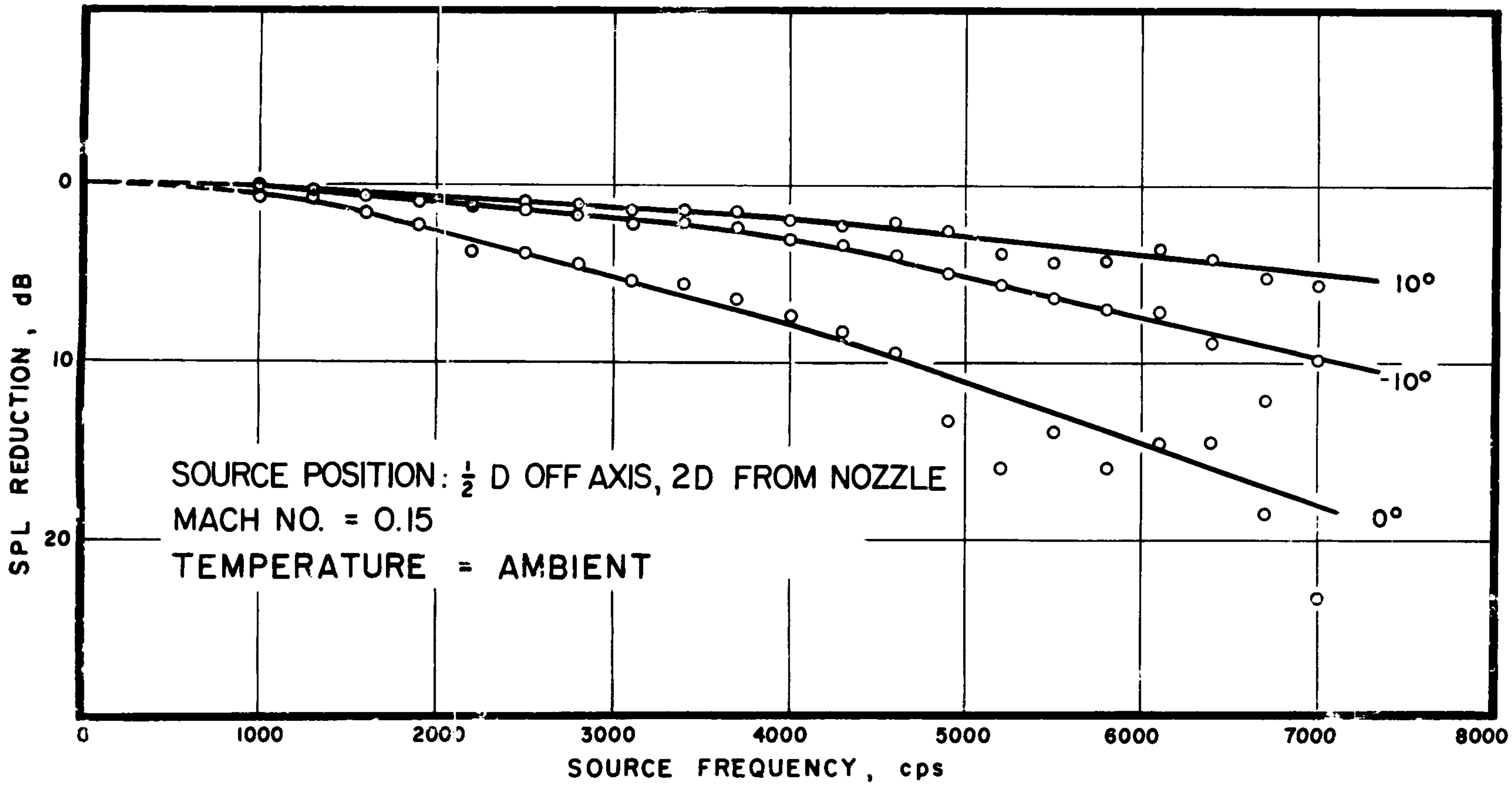

FIG. 13. TYPICAL SPL REDUCTION VS. FREQUENCY CURVES FOR OFF-AXIS SOURCE LOCATION

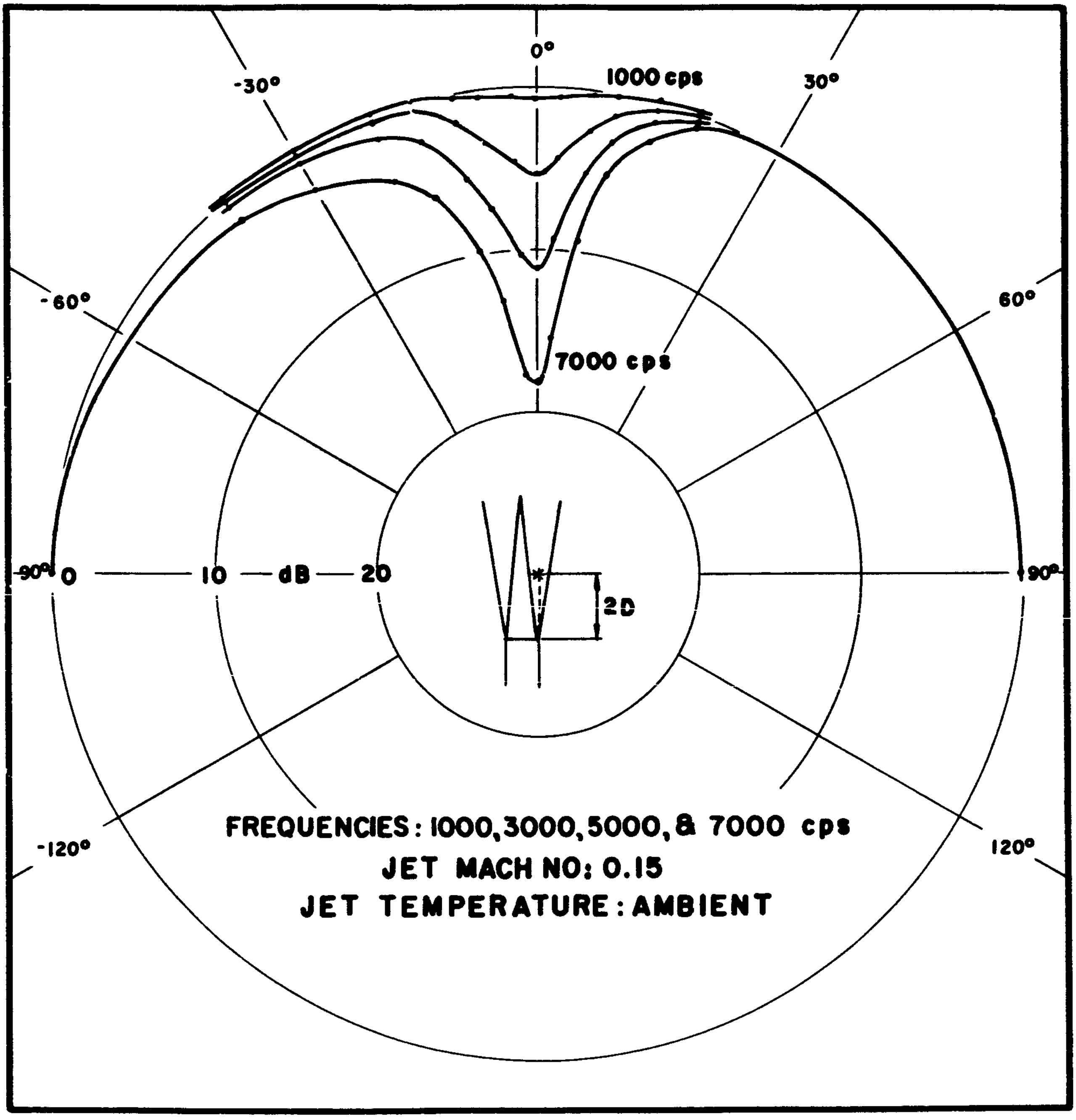

FIG.14. ASYMMETRIC REFRACTION PATTERNS FOR OFF-AXIS SOURCE LOCATION

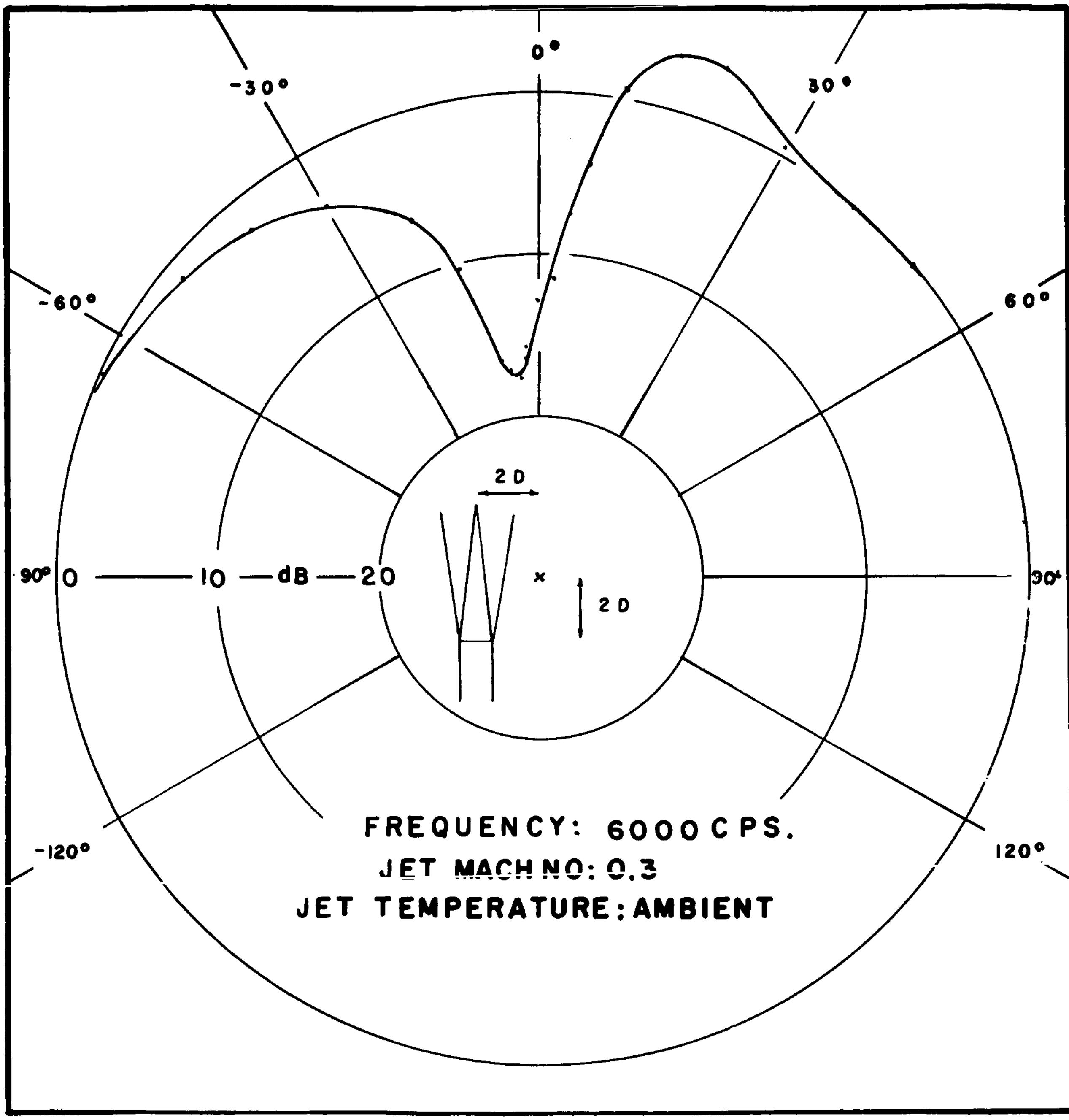

FIG.15. ASYMMETRIC REFRACTION PATTERN FOR OFF-AXIS SOURCE LOCATION

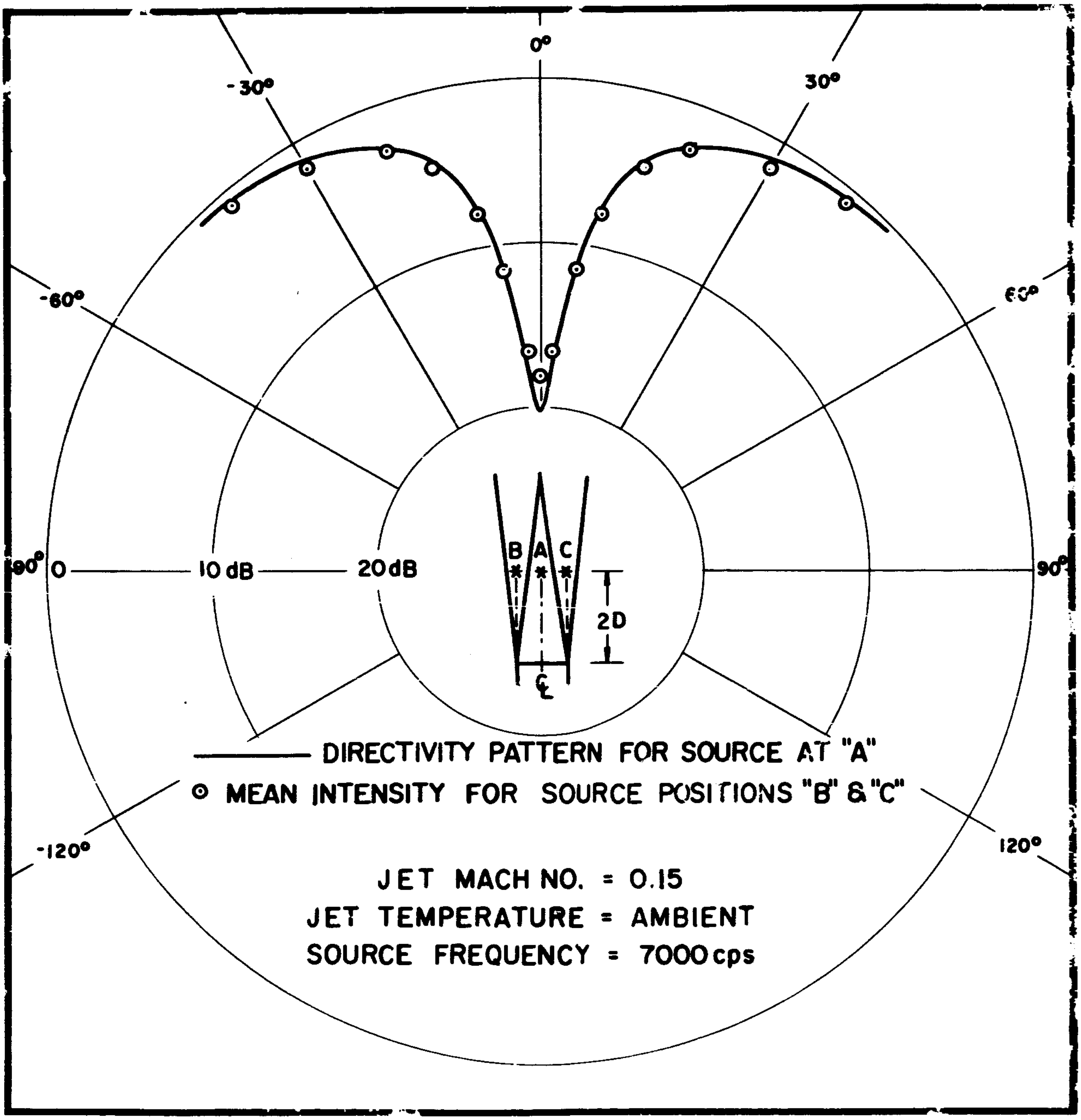

FIG. 16. COMPARISON OF THE AVERAGE INTENSITY DISTRIBUTION FOR TWO SOURCE POSITIONS ON OPPOSITE SIDES OF THE JET AXIS, ½D AWAY FROM THE AXIS, WITH THE CORRESPONDING INTENSITY DISTRIBUTION FOR A CENTRED SOURCE